Streamlined Shape of Endothelial Cells

Chanil Chung
Institute of Medical and Biological Engineering in Medical Research Center, Seoul National University
Jun Keun Chang*
School of Electrical Engineering and Computer Science, Seoul National University
Byoung Goo Min
Department of Biomedical Engineering, Seoul Natiuonal University
Dong Chul Han
School of Mechanical and Aerospace Engineering, Seoul National University

Flow induced shape change is important for spatial interpretation of vascular response and for understanding of mechanotransduction in a single cell. We investigated the possible shapes of endothelial cell (EC) in a mathematical model and compared these with experimental results. The linearized analytic solution from the sinusoidal wavy wall and Stokes flow was applied with the constraint of EC volume. The three dimensional structure of the human umbilical vein endothelial cell was visualized in static culture or after various durations of shear stress (20 dyne/cm^2 for 5, 10, 20, 40, 60, 120min). The shape ratio (width: length: height) of model agreed with that of the experimental result, which represented the drag force minimizing shape of stream-lining. EC would be streamlined in order to accommodate to the shear flow environmented by active reconstruction of cytoskeletons and membranes through a drag force the sensing mechanism.

Key Words : Endothelial Cell, Drag Force, Stream Lining Shape, Cytoskeleton

1. Introduction

Endothelial cells (EC) are exposed to continuous shear stress from their birth and also respond to the hemodynamic changes of their environment which may be a localizing factor in vascular disease such as atherosclerosis. Atherosclerosis has been associated with the genetic disorders and other risk factors such as hypertension, smoking, hyperlipidemia, diabetes mellitus, social stress, lifestyle, viral infection and possible chlamydial infection. Nevertheless atherosclerosis is a geometrically focal disease and has a tendency to occur in blood vessel bifurcations where the blood flow produces complex forces on the vessel wall. It has been shown that the endothelial cells aligne with the direction of blood flow and elongate in a polygonal or ellipsoidal shape. It has been also investigated the relationship between hemodynamic forces and the cellular processes involved in atherogenesis. It is generally accepted that the EC changes its whole morphology in order to reduce shear stresses on the surface of an EC. (Okano and Yoshida, 1992; Barbee et al., 1994; David Ku, 1997; Malek et. al. , 1999). This study analyzes the fluid dynamic force balance between the drag force and the adhesion force of EC to the extracellular matrix.

* Corresponding Author,
E-mail : jkchang@amed.snu.ac.kr
TEL : +82-2-880-1683; **FAX** : +82-2-887-4225
School of Electrical Engineering and Computer Science, Seoul National University, San 56-1, Shinlin-dong, Kwanak ku, Seoul 151-742, Korea.(Manuscript **Received** September 15, 1999; **Revised** June 1, 2000)

2. Methods

2.2 Stokes flow on sinusoidal wavy wall

The endothelial cell monolayer is modeled as a inusoidal wavy wall (Fig. 1). Flow near the ndothelial cell surface is characterized by creeping flow and the momentum transfer is thus overned by viscous forces. The first theoretical ttempt to model the endothelial monolayer as a vavy wall was reported. (Satcher, et al., 1992). hear stress and pressure were normalized with μ /; the mean wall shear stress was imposed by flow ar from the endothelial surface:

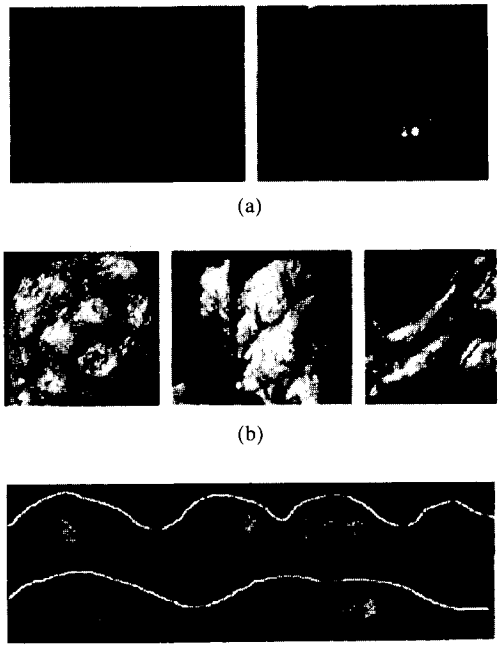

(a)

(b)

(c)

Fig. 1 Sinusoidal wavy pattern of an endothelial monolayer. (a) Fluorescent microscopic view of endothelial cells. (b) Three-dimensional shapes of endothelial cells: PV-WAVE software reconstructed the cell from the Laser Confocal Scanning Microscopy (LCSM) images of z series. (c) Cross-sectional images of endothelial cell: NIH image created vertical cross sectional images from the LCSM images of z series. TMA-DPH stained the phospholipid representing the external membrane

$$\tau^*=\frac{\tau}{\mu\gamma} \quad P^*=\frac{P}{\mu\gamma} \quad Q=\frac{l_y}{l_x} \tag{1}$$

$$\tau^*_{yz}=1+2\pi\frac{2+q^2}{\sqrt{1+q^2}}\frac{h}{l_y}\cos(\alpha x)\cos(\beta y) \tag{2}$$

$$P^*=-4\pi\frac{h}{l_y}\cos(\alpha x)\sin(\beta y) \tag{3}$$

Using this solution, the maximum shear stress and maximum shear gradient can be calculated in terms of the geometric parameters as follows

$$|\tau^*_{yz}|_{\max}=1+2\pi\frac{2+q^2}{\sqrt{1+q^2}}\frac{h}{l_y} \tag{4}$$

$$\left|\frac{\partial\tau^*_{yz}}{\partial y}\right|_{\max}=4\pi^2\frac{2+q^2}{\sqrt{1+q^2}}\frac{h}{l_y^2} \tag{5}$$

In evaluating the effect of endothelial cell shape change under shear flow (Oliver and Truskey, 1993; Fung and Liu, 1993), we assumed that the volume of an endothelial cell was constant (Fig. 2) where a typical EC would change its shape from a sphere to a sinusoidal wavy form. The three geometric parameters can thus be reduced to two and one ratio: volume(V), width (l_x), and the ratio of length/width (q). If the spherical volume is equal to the wavy cell volume, the ratio of width /diameter (p) can determine the initial width (l_x).

$$l_x=p\cdot D \tag{6}$$

$$l_y=q\cdot l_x \tag{7}$$

$$2h=\frac{V}{l_x\cdot l_y/4}=\frac{2\pi D^3}{3l_x^2q} \tag{8}$$

$$(\text{width: length: height})=\left(1:q:\frac{2h}{l_x}\right) \tag{9}$$

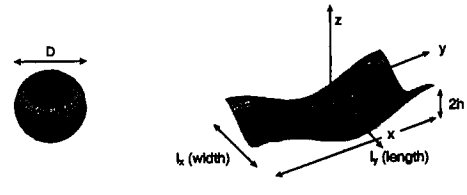

$$V=\frac{4\pi}{3}R^3=\frac{\pi}{6}D^3 \qquad V=\frac{l_x\cdot l_y\cdot 2h}{2\cdot 2}=\frac{l_x\cdot l_y\cdot h}{2}$$

Fig. 2 Volume constrained model of endothelial cell. The wavy model consists of two cells which have the shape of $f=h\cdot\cos(\alpha x)\cos(\beta y)$ where $\alpha=2\pi/l_x$: $\beta=2\pi/l_y$

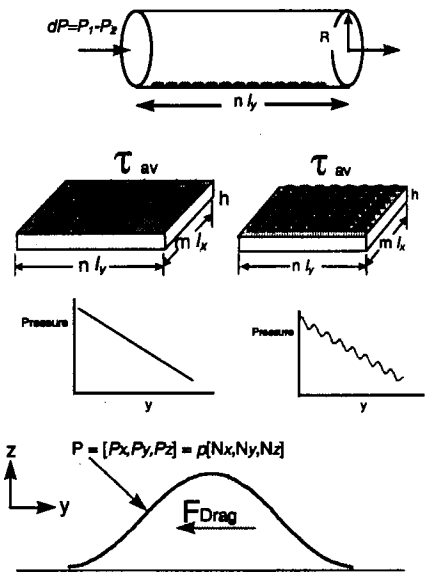

Fig. 3 Pressure drop on the endothelium as plane or wavy wall. τ_{av} is the mean shear stress for the mean pressure drop (dP). The wavy surface profile produces the pressure perturbation over one endothelial cell

The ratio of cell shape (width : length : height) can therefore be defined by three parameters: initial width (l_x), diameter of the sphere (D), and ratio of length/width (q).

2.2 Derivation of drag force

$$P(x, y)=\bar{P}^*+P^* \tag{10}$$

$$\bar{P}^*=\frac{2\cdot l_y}{R}\cdot\left(1-\frac{2y}{l_y}\right) \tag{11}$$

$$P^*=-4\pi\frac{h}{l_y}\cos(\alpha x)\sin(\beta y) \tag{12}$$

Because the radius of a vessel is much larger than the length of a cell, the mean pressure drop $\bar{P}^*$ is relatively smaller than the perturbation term P^*. In our endothelial cell model, pressure deviation creates drag (Fig. 3), in addition to a drag force from the surface shear stress. To calculate the drag force on one cell, the pressure normal to the cell surface was projected in the direction of mean flow (+y axis). The integration of shear stress (τ_{wall}) and flow directional pressure drop (P_y) over the cell area (A, *where* x: $-l_x/2 \sim l_x/2$, y: $-l_y/2 \sim l_y/2$, Fig 2.) gives the total drag force.

$$F_{drag}=\int \tau_{wall}dA+\int P_y dA \tag{13}$$

2.3 Construction of endothelial cell-extracellular matrix system

Human umbilical vein endothelial cells (HUVECs) were isolated using a modified collagenase digestion method and then seeded on the human fibronectin (5 mg/cm^2, Boehringer Mannheim, Germany)-coated micro slide glass. Seeding density was about 5×10^4 cell/cm^2.

2.4 Stress exposure protocols

An experimental setup of a laminar flow chamber for HUVECs adhering to the micro slide glass was developed (Frangos et al., 1985). Shear stress (τ; dyne/cm^2) was calculated by the equation $\tau=6Q\mu$ /bh^2 where Q was the measured flow rate (ml/s) generated by hydrostatic pressure, μ the viscosity (0.01 poise), b the width of the flow channel (1.0 cm), and h its height (0.03 cm). Our previous computational fluid dynamic (CFD) study confirmed the short entrance length (<0.5 cm) and laminar flow over the seeded region of HUVECs that were exposed to a steady laminar flow for different durations. Shear stress was adjusted to 20 dyne/cm^2. As a control, HUVECs were cultured under static condition and the exposure time to the shear stress was 5, 10, 20, 40, 60 and 120 min, respectively.

2.5 Immunofluorescent staining protocols

For the double-labeling of indirect immunofluorescence staining after flow experiments, cells were washed briefly with warm PBS (37°C, pH 7. 4), fixed with 3.7% formaldehyde for 10 min, permeabilized with 0.1% Triton X-100 (Boehringer Mannheim, Germany) for 10 min at room temperature, and incubated in PBS with 1% BSA (Sigma Chemical Co.) for 1 hr blocking. These cells were then stained with 5 μl of rhodamine -phalloidin (Molecular Probe Inc.) for actin microfilaments and with 10mM TMA-DPH (Molecular Probe Inc.) for phospholipid membrane for 30 min, and mounted with a solution of 30% glycerol and 0.1% sodium azide in PBS.

With TMA-DPH for membrane phospholipid marker and rhodamine-phalloidin for actin microfilaments, laser scanning confocal microscopy (LSCM) generated the sliced images of z scanning. PV-WAVE software was used to produce the volume rendered images of the cell surface. (Fig. 1)

3. Results

The surface distributions of different flow forces including pressure and shear stress are shown in Fig. 4. Two different cell topographies show that the elongated and height reduced models have smaller magnitudes of flow characteristics than the reference models. To date, the maximum shear stress and shear stress gradient have been the best indicators that describe the shape change of endothelial cells under flow condition. However, this model can evaluate other parameters, as shown in Fig. 5, which indicates that the integrated net shear and the drag force, each has a local minimum at certain reference widths and heights. Morphologic changes in ECs caused by flow force can be summarized as follows: i) from a cobblestone-like shape to an elongated rugby-ball like shape; ii) the reduction of cellular height (from 8.12 ± 0.83 μm to 5.46 ± 0.51 μm); iii) the formations of lamellipodium and focal contacting area; iv) the reorganization of actin microfilaments from thin filaments to thick ones, including the bundling and formation of stress fibers. In particular, the volume of cells subject to shear remains unaffected by flow duration (ANOVA test: $P<0.0001$). This agrees with the previous assumption of constant volume in our mathematical model (Fig. 6). The simulated and experimental results were compared; the

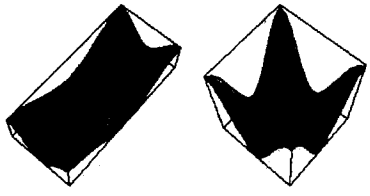

(a) Pressure

(b) Flow directional shear

Fig. 4 Surface distribution of various parameters. (a) pressure, and (b) flow directional shear. The color scale was adjusted to visualize differences in the magnitude of the surface

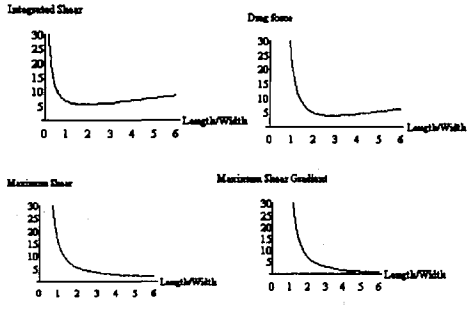

Fig. 5 The normalized simulation results of the fixed model height and width. Local minimums exist in drag force and net shear

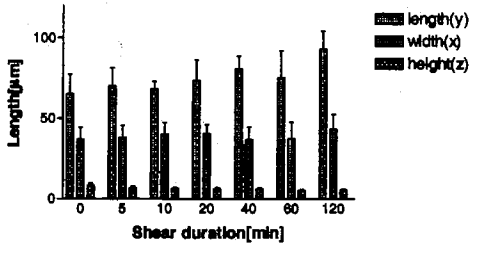

(a)

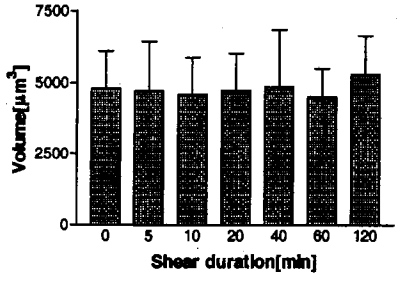

(b)

Fig. 6 Time history of (a) length, height, width, and (b) the volume, of shear (20dyne/cm^2) exposed endothelial cells. ANOVA test indicated that the volume was not affected by shear duration time ($P<0.0001$)

Table 1 Comparison of model estimation and experimental results

Condition	Width/ Reference length	Width:	Length:	Height
Estimation by sinusoidal wavy endothelium model with minimal drag force	1.2	1	2.172	0.278
	1.4	1	1.749	0.218
	1.6	1	1.922	0.176
Static culture	1.372	1	1.764	0.231
Shear(20dyne/cm^2) for 120 min	1.540	1	2.141	0.127
Shear(45dyne/cm^2) for 120 min	1.610	1	1.963	0.125

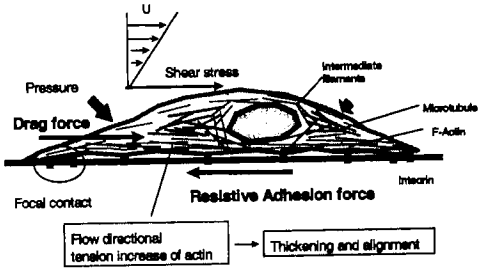

Fig. 7 Drag force-mediated force transmission to actin cytoskeleton network

width normalized by the reference length (l).

$$l=\sqrt[3]{l_x \cdot l_y \cdot h} \tag{14}$$

Table 1 compares the model estimations with the experimental results. It illustrates the possible shapes of an endothelial cell under shear flow based on the minimal drag force and shows the general agreement between the model and the experiment.

4. Discussion and Conclusion

The fluid dynamic force balance on an endothelial cell in the blood vessel wall could be a factor in its topology. The focal contact of the integrin complex, which consists of substratum, integrin receptor, and actin microfilaments, could possibly sense the drag force of fluid flow through certain mechanisms such as conformational change similar to the force transmission apparatus of a lever. At the contact point, the intracellular tension of actin microfilaments increases, inducing its polymerization. The actin cytoskeleton consequently grows into F-actin along the direction of the drag force. (Fig. 7). This implies that the formation of F-actin and the subsequent morphologic changes are directly affected by the flow force applied not only to the upper membrane but at the focal adhesion complex where the force information is transmitted to the cytoplasm through the network of the cytoskeleton. The morphology of an EC is possibly reflected by the drag minimizing streamlined shape rather than shear stress alone.

Acknowledgements

This work was supported by the Ministry of Education through Inter-university Semiconductor Research Center (ISRC 97-E-4034) in Seoul National University

References

Barbee K. A., Davis P. F., and Lal R., 1994, "Shear Stress Induced Reorganization of the Surface Topography of Living Endothelial Cells Imaged by Atomic Force Microscopy," *Circ. Res.*, Vol, 74, pp. 163~171.

David Ku, 1997, "Blood Flow in Arteries," *Annu. Rev. Fluid Mech.* Vol, 29, pp. 339~434.

Fung Y. C. and Liu A. Q., 1993, "Elementary Mechanics of the Endothelium of Blood Vessels," *J. Biomech. Eng.* Vol, 115, pp. 1~12.

Frangos A., Eskin S. G., McIntire L. V., Ives C. L., 1985, "Flow Effects on Prostacyclin Produc-

tion by Cultured Human Endothelial Cells," *Science*, Vol, 22, pp. 1477~1479.

Malek A. M., Alper s. L. and Izumo S., 1999, "Hemodynamic Shear Stress and Its Role in Atherosclerosis," *J. American Medical Associ.*, Vol, 282 No, 21, pp. 2035~2042.

Okano M. and Yoshida Y., 1992, "Endothelial Cell Morphometry of Atherosclerotic Lesions and Flow Profiles at Aortic Bifurcations in Cholesterol fed Rabbits," *J. Biomech. Eng.*, Vol, 114, pp. 301~308.

Oliver L. A. and Truskey G. A, 1993, "A Numerical Analysis of Forces Exerted by Laminar Flow on Spreading Cells in a Parallel Plate Flow Chamber Assay," Biotechnology and Bioengineering, Vol, 42, pp. 963~973.

Satcher R. L., Jr., Bussolari S. R., Gimbrone M. A., Jr., and Dewey, C. F. Jr., 1992, "The Distribution of Fluid Forces on Model Arterial Endothelium Using Computational Fluid Dynamics," *J. Biomech. Eng.*, Vol, 114, pp. 309~316.